Deep Brain Magnetothermal Silencing of Dopaminergic Neurons via Endogenous TREK1 Channels Abolishes Place Preference in Mice

Junting Liu[1], Rahul Munshi[1], Muye He[1], Sara D. Parker[1], Arnd Pralle[1,*]

[1]Department of Physics, University at Buffalo, the State University of New York, Buffalo, 14260, New York, USA

*: Correspondence should be addressed to A. P. (apralle@buffalo.edu)

Highlights

- TREK1 is a highly efficient, thermally activated neuronal silencer
- First magnetothermal neuronal silencing in behaving mice
- Fiber photometry determination of local heating and silencing of target neurons in the ventral tegmental area
- Magnetothermal suppression of dopaminergic reward response in the ventral tegmental area is sufficient to abolish place preference

Abstract

Reversible silencing of neuronal activity in freely behaving animals provides a powerful tool to determine the roles of specific neuronal populations in circuit dynamics and behavior. Here, we show how magnetothermal silencing using endogenous TREK-1 channels can suppress the dopaminergic reward in the ventral tegmental area and the place preference in mice.

Magnetothermal silencing uses alternating magnetic fields penetrating tissue undiminished without harmful effects to heat superparamagnetic nanoparticles at the target cells. The induced sudden, small increase in temperature inhibits neuronal firing rapidly and reversibly, and without the need of genetic modification of the neurons. We demonstrate that two-pore potassium channel TREK-1 channels are responsible for this thermal neuronal silencing. Using fiber-based optogenetics we measure the heating and neuronal silencing in the ventral tegmental area (VTA) brain of the animals. We show that in a place preference assay magnetothermal neuronal silencing of the dopaminergic neurons in the VTA is sufficient to abolished the place preference. TREK1 knock-out mice are immune to the magnetothermal silencing and behave as if the magnetic field were not applied.

Introduction

Given the choice between a dark and a bright room, rodents innately prefer to remain in the dark. The choice may be driven by an aversion or fear of the bright area, a positive reward when entering the dark, or a combination of both signals. The most direct way to determine with signaling activity drives the choice is transiently silence specific neuronal signaling during the behavior.

In the past decade, various optogenetic[1] and chemogenetic[2] silencing tools have been developed and applied to isolate the role of specific neuronal populations[3]. The quick onset and short duration og optogenetic neuromodulation is excellently activation[4]. However, neuronal silencing needs to persist for the duration of behavior or sensory input which may continue for tens of seconds. Prolonged optogenetic silencing exposes the neurons to potentially damaging high light intensity for an extended time. Chemogenetics provides longer persisting neuromodulation, minutes to hours, even days and weeks. However, chemogenetic modulation is not sufficiently transient to be precisely timed with a particular behavior. Instead, chemogenetics alters the brain circuit for the entire duration of an experiment[5]. We and others have shown that magnetothermal-genetic activation provides neuromodulation at a time scale ideally suited for silencing[6,7]. Other advantages are that approach is tetherless, large or multiple brain regions can be targeted easily, and the position of the external magnetic field defines the location of the stimulation within the experimental arena. We recently showed that the chloride channel ANO1/TEM16A may be used for magnetothermal silencing of neurons in culture[8]. Here, we demonstrate the first magnetothermal neuronal silencing in behaving mice using the potassium leak channel TREK1.

The two-pore (K2P) channel TREK1, a TWIK - related potassium channel[9], is not only is mechanosensitive[10,11] but also thermosensitive[12]. Prior work showed that overexpressing a constitutively active TREK1 channel silences hyperactive neurons and ameliorates epileptic seizures[13]. Therefore, TREK1 channel should be suited as a thermal silencer for neuronal activity[12]. TREK1 is expressed in the central nervous system (CNS), cortex, dorsal root ganglia (DRG), and hippocampus. Generally, high expression levels are found throughout the midbrain, although the expression is moderate in the ventral tegmental area (VTA). Recently, TREK1 channels have been identified to be involved in various phenomena: volatile anesthetics modulate TREK1 channel activity[14], TREK1 is involved in depression[15] and in glutamate release in astrocytes[16].

We applied magnetothermal neuronal silencing to study whether silencing of a dopaminergic reward alone suffices to erase the choice preference in a decision-making assay. Conditional place preference between a dark and a well-lit room was used simple decision paradigm. Magnetothermal neuromodulation is particularly well suited for that assay as the magnetic field can be applied to just one of the rooms directly

correlating stimulation with the animal's location. Also, the duration of the animal in one location correlates preferably with the temporal resolution of magnetothermal neuronal silencing.

Results

Entering the dark room in a light/dark chamber causes the activation of dopaminergic neurons in the ventral tegmental area

We hypothesized that the innate preference of rodents for the dark chamber in a light/dark test may be less an aversion of the brightly illuminated areas as mild stressor[17], but at more the result of a positive reward response upon entering the dark room. To determine whether a positive reward response occurs upon entering or remaining in the dark area we studied the activity of dopaminergic neurons (DA) in the ventral tegmental area (VTA) of mice. First, we examined the neuronal activity of mice either roaming in an evenly brightly lit arena or in an arena equally split into a dark and a light room (Fig. 1 A - D). Post-experiment c-Fos staining showed a significantly raised number of active neuron in the VTA for the mice in the dark/light chamber compared to the animals in the light-only chamber. The total number of cells and dopaminergic neurons were the unchanged (DAPI and TH stains in Fig. 1 D). The majority (65%) of neurons in the VTA brain area are dopaminergic[18]. Detailed analysis of the C-fos positive neurons revealed that the vast majority were dopaminergic, TH-positive neurons (86% overlap) and that the activity in GABA-positive neurons was unchanged (Suppl. Fig. S1). This data suggests demonstrates that having access to a dark room during the experiment leaves the imprint of a positive reward in the animal's VTA.

To determine the temporal correlate between entering a particular room and the reward onset, we used optical read-out of VTA neuronal activity. The neuronal activity was measured via fiber-photometry in animals over-expressing GCaMP6s in the VTA while the animals explored an equally split into a dark and a light room (Fig. 1 E). The recordings show that as soon as the animals enter the dark region the neuronal activity in the VTA increases, reaching a peak about one second after entering the dark region. The kinetics and dynamics of the increased activity are the same in WT as well as in TREK1 KO animals (Fig. 1 F). Further quantification shows about 2.5-fold activity increase in both animal groups (Fig. 1 G, activity during 0.35s to 2.15s versus -2.15s to -0.35s). When the animal moves in the reverse direction, from dark to light, the photometry recording showed a gradual decrease of neuronal activity in the VTA back to the baseline level (Suppl. Fig. S2).

Together, these data support the idea that a reward response in the VTA contributes to the preference of the dark over the light room in rodents. Deciphering any causality of this signal to the behavior requires suppressing this pathway.

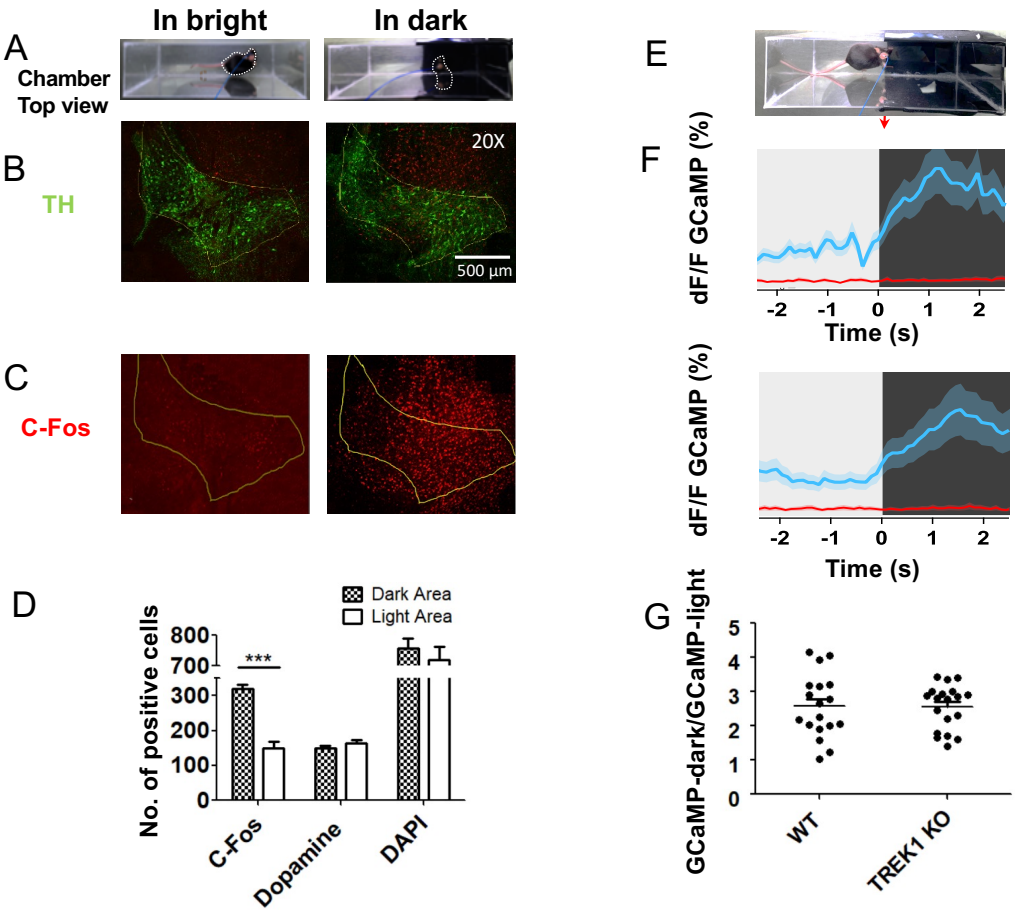

Figure 1: Entering the dark in a dark/bright assay activates dopamine neurons in the ventral tegmental area.

(A) Light-dark behavior chamber setup schematic, place-preference assay for intrinsic preference of dark space. Half chamber is dark, and another half is bright chamber. **(B)** Representative TH/C-Fos staining in the lateral VTA profile for mouse dwelling in dark and bright area, scale bar 500 µm. **(C)** C-Fos staining for active neuron during assay: the animal remained in either light or dark arena for 20 min. **(D)** The quantification of DAPI staining of cell nuclear in both dark and bright areas, and the quantification of dopamine neurons (TH staining) number both dark and bright areas. Based on the similar quantification of the nuclear and dopamine cell number in the ROI, The significant quantitative analysis of the different numbers of positive cell number in the same lateral ROI area for a relatively long duration of the mouse the dark and bright area. (***P<0.001, n = 15 from 3 mice/group). **(E)** Animal with implanted fiber in light-dark chamber. **(F)** Peri-event plot of averaged calcium signals recording via fiber photometry during bright to the dark area for instant state change (2.5s bright and 2.5s dark area), solid line and the shaded region are the mean ± s.e.m. (n=3 bouts from 2 WT mice). **Top:** Wild-type animals. **Bottom:** TREK1 knock out animals. **(G)** Summary of dark/light activity from WT and TREK KO animals. Bar plots show the significant change during the state change from dark to bright or reversible bright to dark process, mean ± s.e.m. (***P<0.001, n = 3 from 2 mice/group).

112 **The TREK1 channel is a fast and strong thermally activated neuronal silencer**

113 To suppress the neuronal activity in the VTA while in the dark room, we developed magnetothermal
114 neuronal silencing. Previously, we developed magnetothermal silencing using the chloride channel
115 TMEM16A[8]. We chose not to use that approach in-vivo because extra chloride influx challenges the health
116 of the neurons and the size of TMEM16 is difficult for viral packaging. Instead, we used the potassium leak,
117 two-pore channel TREK1. Expressing a constitutively active TREK1 channel in regions of the CNS has
118 been shown to silence hyperactive neurons and to ameliorate epileptic seizures[13]. As TREK1 is mildly
119 thermosensitive[12], we hypothesized that combining TREK1 with remotely heating magnetic nanoparticles
120 would create a strong and safe magnetothermal neuronal silencer.

121 To determine whether thermally activated TREK1 would hyperpolarize neurons sufficiently to suppress
122 their activity, we over-expressed TREK1 in cultured hippocampal neurons (TREK1 OE). Exposing the cells
123 to temperature ramps from 34°C to 42°C, we observed that the neuronal spiking measured via GCaMP6f
124 fluorescence subsided as soon as the temperature ramp began (Fig. 2 A, rate of temperature increase
125 0.15 °C/s). Silencing occurred even at bath temperatures below physiologic temperatures. During the
126 cooling phase, the firing of the cells resumed around physiological temperatures.

127 TREK1 is normally expressed in various regions of the central nervous system. High expression levels are
128 found throughout the midbrain, with moderate expression in the VTA, good expression in the hippocampus,
129 the cortex, and dorsal root ganglia. Figure 2 B shows that endogenously expressed TREK1 in hippocampal
130 neurons suffices as a thermal silencer. The response was slower and slightly weaker than in neurons
131 overexpressing TREK1. The pooled data of several cultures demonstrates that applying a positive
132 temperature ramp reduced the number of calcium spikes in WT and TREK overexpressing hippocampal
133 neurons 5- to 6-fold (Fig. 2 C). In TREK1 overexpressing cells, the temperature ramp efficiently silences
134 neurons even at temperatures below physiological temperature, but only in combination with a positive
135 temperature ramp (Fig. 2 D).

136 Our data showed that neuronal firing is suppressed as soon as the temperature ramp begins. The delay
137 between the start of heating and onset of silencing is 0.9 seconds (n= 13) for TREK1 overexpressing cells,
138 then ~3 seconds (n=7) for the WT neurons. As the rate of temperature increase was 0.15 °C /s, then neurons
139 are silenced before the temperature has risen 0.15 °C in TREK1 overexpression cells, and less than 0.5 °C
140 in WT neurons. This is faster than magnetothermal activation using TRPV1 and sufficiently fast to yield
141 good temporal correlation with behavioral changes.

142 The principle of the magnetothermal silencing is shown figure 3 E: superparamagnetic nanoparticles coated
143 with antibodies against a neuronal epitope bind to the membrane of the target cells expressing TREK1.

Upon application of the alternating magnetic field the particles dissipate hysterical losses as heat to the environment. The activated TREK1 channels increase the potassium efflux and hyperpolarize the cells.

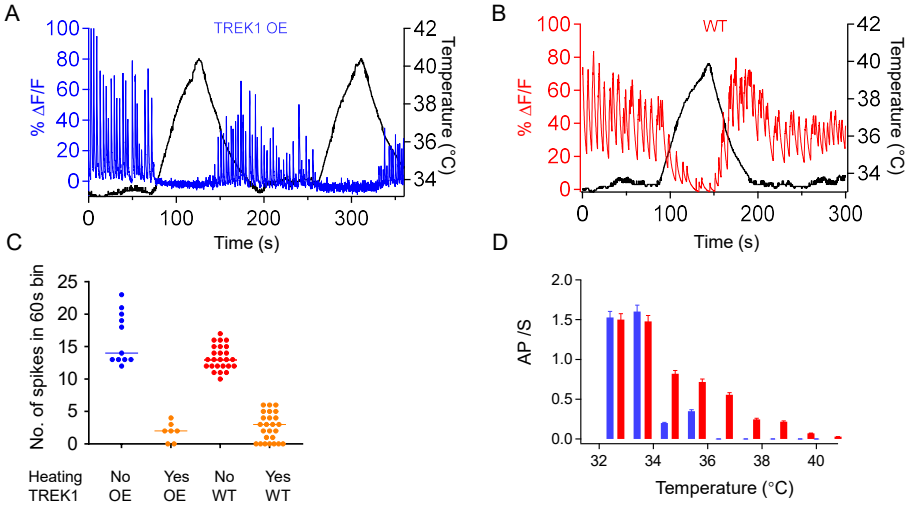

Figure 2: The TREK1 channel is a fast and potent thermally activated neuronal silencer.

(A) Normalized GCaMP6f fluorescence signal showing silencing of TREK-1 overexpressing (OE) rat hippocampal neurons with positive temperature transients (0.15 °C/s). **(B)** Normalized GCaMP6f fluorescence signal showing silencing of wild-type (WT) rat hippocampal neurons with bath temperature ramp (0.15 °C/s). **(C)** TREK1 overexpressing neuron's activity as spikes per firing spike numbers per minute without heating (blue, n=11) and spikes per minute during a heating period (heating rate: 0.15 °C/s, n=5). WT neuron's firing frequency as spikes per minute without heating (red, n=25) and WT cell's spikes per minute during the heating (heating rate: 0.15 °C/s, orange, n=24) (Solid thin mid-line and the top-down thick lines are the mean ± SEM,. *** $p<0.001$, two-way ANOVA between without heating and with heating). **(D)** Action potential (AP) rate of WT (red) and TREK1 overexpressing (blue) cultured neurons temperature at difference absolute temperatures (0.15 °C/s heating rate).

In vivo magnetothermal heating

Magnetothermal neurostimulation in vivo requires fast, precise and controlled heating of a few cells deep in the brain. The heating was achieved by injecting super-paramagnetic nanoparticles near the targeted cells.

The local temperature at submicron scale may be measured using optical photometry, using the temperature dependence of the fluorescence lifetime of fluorophores[6,19]. We used photometry to determine the temperature at the nanoparticles and at the target neurons in the VTA inside the living animals directly. The temperature measurement at the surface of the nanoparticles used the fluorophore embedded in the polymercoat of the MNPs, DyeLight 550 (Fig. 3 C). As the temperature rises, the fluorescence intensity decrease. Using the calibration curve for a particular fluorophore, it is possible to calculate the actual

168 temperature at the MNPs (Fig. 3 C). To quantify the temperature within the target neurons, we used the
169 fluorescence of the expressed GCaMP7f (Fig.3. D).

170 The corresponding temperature increasing and decreasing curve (Fig.4 c right and Supplementary
171 Information Fig.6 d bottom) showed controllable temperature manipulation in the deep brain in small
172 animals with an accurate stereotactic injection, however, it is not limited to small animals in the future.
173 While low-radiofrequency alternating magnetic fields (AMFs) enable penetration into the body without
174 substantial attenuation and thus allowing signal delivery into the deep brain without a major loss of depth
175 penetration[20], then the AMFs in this study (22.4 kA/m at 412.5 kHz, also adjustable) can be converted into
176 biological tissue heating depending only on the magnetic field used in the hyperthermia experiments and
177 the MNPs magnetization[21]. The GCamp7f will be stably expressed after it was laterally injected with 0.5 µl
178 Gcamp7f (*AAV9.syn.flex.jGCamp7f.WPRE.SV40*) for four weeks of transfection, which was followed by
179 implanted fiber on the above expression area, the VTA expression profile (Fig.4 a left and Fig.4 a right:
180 partially enlarged view of VTA), and fiber track (Fig.4 a right), and then the mouse was given an MNPs
181 angle injection into the same region (Supplementary Fig.6 a, b, c). There are two kinds of MNPs heating
182 patterns: an accurate bulky volume stereotactic injection into the VTA (Supplementary Fig.6 c). The
183 magnetothermal heating effects are injected volume dependent (Supplementary Fig.6 e); this method allows
184 the MNPs to reside in the location for 1-2 months, and another pattern is bound to the membrane for special
185 neurons' population with antibodies, which is particularly important as it enhances the specificity of
186 stimulation confining the effect to the targeted cells without any spillover to the neighboring tissues. For
187 the *in vivo* mouse local heating experiments, the anesthetized mouse/freely moving mouse was exposed to
188 the magnetic field conditions, and the mouse head was located in the central height of the coil described
189 above. The magnetic coil maintained a stable temperature by circulating cooling water (Fig.1 Right ellipse);
190 in addition, in order to keep the mouse comfortable, 36 °C constant temperature water was placed in one
191 plastic container to insulate the heat radiation from the coil (Fig. 1 right cross-sectional view blue circle).
192 The slope of the integrated GCaMP7f signal was collected and analyzed during three distinct time periods:
193 one prior to AMF application (baseline fluorescent intensity around 36 °C), one during magnetothermal
194 heating (with temperature > 37 °C), and a final period when the local heating temperature resumed to
195 baseline levels. We observed that the temperature increased 6.5 °C from 36.0 °C to 42.5 °C with 60 s AMF
196 heating and bulky volume injection of MNPs (Supplementary Fig.6 d); the histology of the volume angle
197 injection showed yellow MNPs in the VTA brain region and VTA profile (Fig.4 a). Another kind of MNPs
198 injected and binding the membrane of neurons showed a similar temperature increase of 5.6°C from 36.2 °C
199 to 41.8 °C (Fig.4 c). On the other hand, the local temperature increasing in the vicinity of the MNPs was
200 measured by fluorescence intensity changes of DyeLight 550 fluorophore integrated in the NeutrAvidin
201 coating for the membrane binding pattern. The DyeLight 550 binding with the MNPs showed the MNPs

distribution and the relative position with the VTA profile (TH staining for dopamine neurons) (Fig.4 a). The fluorescence intensities of molecular fluorophores are sufficiently temperature-dependent to provide a molecular scale thermometer in our previous research[19]. Also, we examined the antibody bonding to membrane heating in the mouse motor cortex as well, where the heating consistent with other brain regions and curves showed ~5.5°C increase and the heating temperature was from 36.3°C to 41.8 °C. Generally speaking, our *in vivo* local heating showed around 5.5 to 6.5-degree temperature increase in both the deep brain and in the VTA (~4.2-4.8 mm) or shallow area (~1.5 mm) in the motor cortex, and this heating is not dependent on the depth of the MNP injection, thus the heating is enough to activate thermosensitive ion channels for neural activation or suppression during 60s or any duration time with the field on, and the heating temperature can be adjusted by different field durations with the same AMF frequency or different field durations and different AMF amplitudes, or even different magnetic field parameters and MNP parameters. More importantly, we realized accurate local heating and *in vivo* measurements for the first time in a mammal.

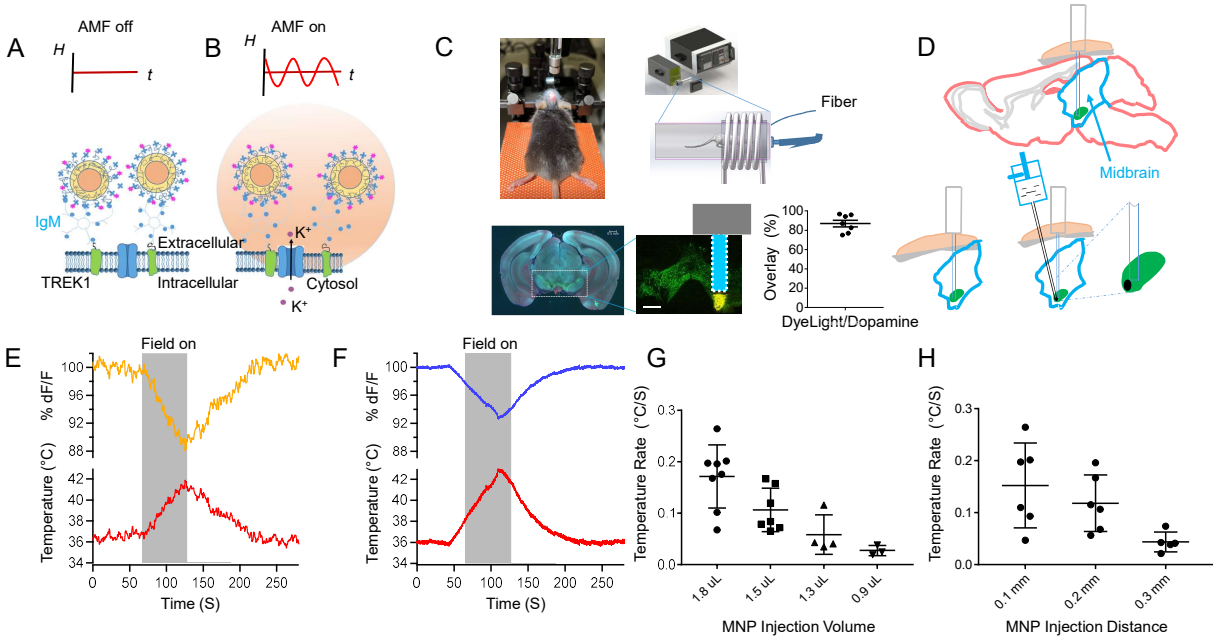

Figure.3: *in vivo* Magneto-thermal heating with Nanoparticles

(A) Alternating Magnetic Field (AMF) stimulation "Field off" of TREK1 without MNP heating is no significant K^+ flowing out the cell, correspondingly, no change of neuron's activity.

(B) The membrane was heated with MNPs upon applying AMF stimulation "Field On" of TREK1, K^+ flowing out the cell, the neuronal activity decreased, and thermal neuro-silencing happened with TREK1 ion channel heating. **(C)** Top row left: Stereotactic injection of GCaMP6s Virus. Top row right: Schematic diagram of the relative position of the magnetic induction coil and the anesthetized mouse, a custom build, water-cooled coil driven by a power supply, the coil has five turns. The mean magnetic flux density along the mouse is 22.4 kA/m at 412.5 kHz for all the heating experiments. The head of the mouse is approximately in the middle of the coil turns. Bottom row left: VTA profile distribution in the whole brain slice of the coronal plane. Bottom row middle: partially enlarged view of the entire VTA area in the white rectangle of left plot, dashed white rectangles indicate fiber location, the yellow area indicates MNPs distribution, scale bar indicates 400 μm. Bottom row right: The percentage of DyeLight 550 (antibody bound the nanoparticles) divides the total number of the dopamine neurons. **(D) Top:** The implanted fiber relative location targets to the bottom part of the VTA brain region. **Bottom**: Bulky injection of MNPs with angle direction beside the implanted fiber and the partially enlarged view of the injected MNPs in the VTA region. **(E) Top curve:** direct measurement of fluorescence change (orange signal) for the DyeLight 550 signal bound with an antibody with the nanoparticles in VTA for *in vivo* mouse. **Bottom curve:** the change in absolute temperature (red signal) corresponding to the change in fluorescence with the calibration factor 1/2.02 of fluorescence change. These temperature measurements are from nanoparticles bound with antibodies. **(F) Top curve:** direct measurement of fluorescence change (blue signal) for the Gcamp6s signal of dopamine neurons in VTA for *in vivo* mice. **Bottom curve**: the change in absolute temperature (red signal) corresponding to the change in fluorescence with the calibration factor 1/1.04 of fluorescence change. These temperature measurements are direct from neurons with the bulky injection of MNPs around the neurons. **(G)** For the bulky injection of MNPs, the heating effects with different injection volumes and ~0.15 mm distance. **(H)** For the bulky injection of MNPs, the heating effects with different injection distance and volume range 1.3-1.5 μL.

Acute *in vivo* magnetothermal silencing of VTA Reward Response

We next sought to determine whether magnetothermal silencing works for acute silencing of the neurons in the VTA for *in vivo* freely moving mice activated by applying ethanol or social interactions. To assess the effects of acute magnetothermal silencing, the mouse was located in the vertical coil and was recorded by fiber photometry. Correspondingly, the process includes the baseline, applying ethanol and magnetothermal silencing, and waiting for a while to recover from the silencing. From the recording data, we dramatically observed the activation of applying ethanol (green background area), and as soon as the AMF was applied, the neurons were immediately inhibited (gray background area) in Figure.5 a; The neuron's activation state was recovered from the silencing which is shown in Figure.5b which was observed around 20 minutes after ethanol activation. The quantification results of basal ethanol activation, acute silencing, and recovery from the silencing are shown in figure 5.c.

On the other hand, in order to confirm the typical acute silencing effect from the social interactions, we customed a social interaction chamber with a satellite chamber connected with a channel; there was a vertical coil and subject mouse inside the central chamber, and it can be visualized along with the social interactions when the same gender stranger mouse walks close to the subject one (Fig. 5 d). The GCaMP6f (AAV5.Syn.GCamp6f.WPRE.SV40) calcium signal shows a dramatic jump during the social interactions when the stranger mouse walks close to the subject mouse (Figure 5.e). Our recording data suggested that

the jumped signal of social interaction and the signal response to the social behavior are repeatable (Figure 5. f). In contrast, we immediately performed the magnetothermal silencing when the stranger mouse walks close to the subject mouse during the social interactions. We found the process did not provide significant GCaMP6f calcium signal jumping (Figure 5.g). The quantification results suggested that our acute silencing has significant effects on social interactions. Therefore, we can condlude that both of these kinds of acute silencing results reveal that our magnetothermal silencing strategy is effective based on the TREK1 temperature-sensitive ion channel.

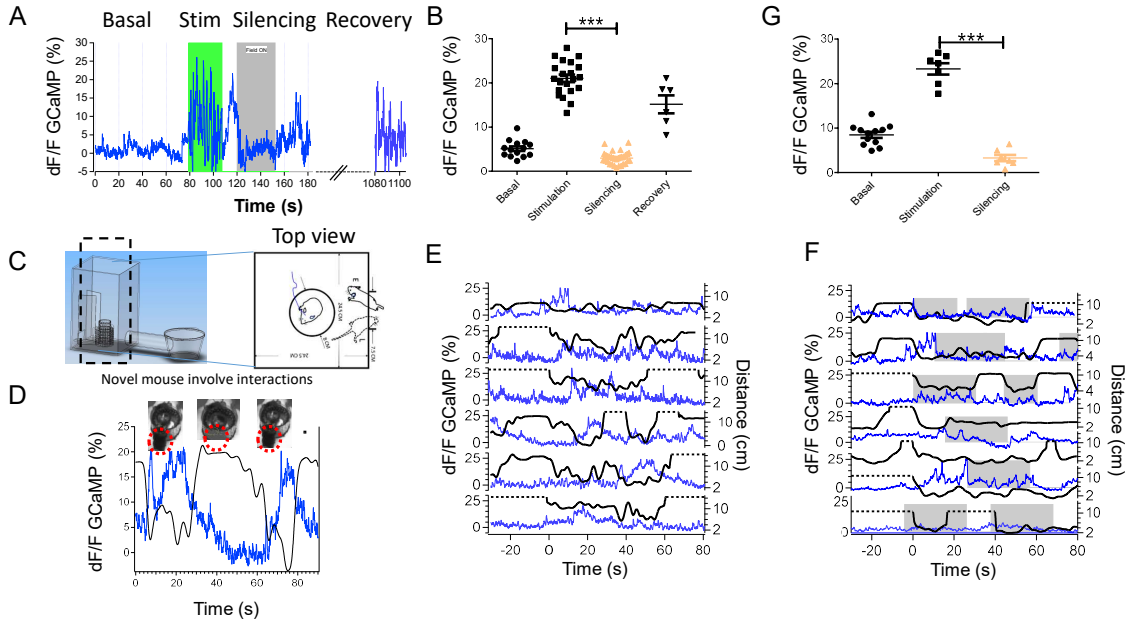

Figure 4: ***In vivo magnetothermal silencing based on reward circuits in VTA***

(A) Representative GCaMP6s fluorescence changes of neuronal activity of the basal, ethanol activation stimulation, and acute magnetothermal silencing with fiber photometry recording in real-time (4 traces from 2 mice). Typical neuronal activity of VTA dopamine neurons recovery of post 15 minutes of silencing duration. **(B)** Quantification of scatters plot of different neuronal activity states: basal, ethanol activation stimulation, magnetothermal silencing, and recovery in the acute ethanol stimulation. **(C)** Left: schematic diagram of magnetothermal stimulation social interaction chamber with a satellite launch room, the recorded mouse located in the vertical chamber in magnetic coil, and another same-gender novel mouse release in the satellite chamber. Right: schematic diagram of video tracking the trajectory of the mouse. **(D)** The typical mouse appears in front of the mouse recorded by Fiber photometry and the real-time Neurons' activity signal without the mouse's social stimulation**. (E)** Multiple mice can repeat the signal activation of the neuronal population in the VTA brain region after typical social stimulation in mice. **(F)** Typical magnetothermal silencing the signals during the social stimulation in the gray shadow magnetic field on durations. **(G)** Quantification of scatter plot of different neuronal activity states: basal, social interaction stimulation, magnetothermal silencing in the acute ethanol stimulation.

Abolishes dark preference through TREK1 silencing and targeting the VTA reward circuit with magnetothermal stimulation

To determine if TREK1 involves a silencing neuronal activity response during magnetothermal stimulation for free moving mice, we further investigated the CPP behavior response with magnetothermal heating. Our light/dark chamber consists of a small dark compartment (one third) and a large illuminated aversive compartment (two thirds), the classic light/dark behavior chamber[22], and the AMF coil setup schematic is shown in Supplementary information Figure.5; this test is based on the innate aversion of mice to brightly illuminated areas. Transitions have been reported to be an index of activity exploration because of habituation over time[17]. The time spent in the dark compartment to be a reflection of the VTA reacting to aversive light illuminated stimuli or dark preference by transient neural activity change. These effects remain unclear whether this reaction directly induces aversive responses in mice behavior through TREK1 activating the neurons' silencing via magnetothermal heating in the temperature-sensitive ion channel. However, we have known that the CPP light/dark chamber test showed the mice changed their behavior and spent more time in the light area after decreasing dopamine neuron population activity in the VTA area with Adiponectin modulation[23]. We know that dopamine (DA) transmission from the VTA is critical for controlling both rewarding and aversive behaviors. Therefore, we hypothesize that CPP behavior will show mice spent more time in the light area after TREK1 was involved in the silencing of dopamine neuron activity. In this study, we examined it by using different expression levels of TREK1 mice in the VTA. Two groups of mice performed the CPP behavior experiments. One group was WT mice, which had a relatively high TREK1 expression in the mouse central nervous system (CNS) and VTA area (Fig. 3 g and h). One third of the behavioral area is darkened and covered by the AMF coil. The mouse is freely moving in and out of the dark compartment and remains in the light/dark chamber for 20 min per trial; the first 5 minutes was performed without the field on, and then the following 10 minutes was performed from minutes 5-15 with the Field on, and the last 5 minutes was performed without the field on again. The percentage of time was spent in the dark place preference chamber inside the coil. The assay was performed twice daily (12- hour interval) before (with the magnetothermal field on and without MNPs injection; no heating) and after nanoparticle injection (with magnetothermal field on and with MNPs injection; has heating) for WT mice (n=10), TREK1 KO mice (n=9), scatter spot plots are shown in WT mice in Fig. 4 e and f at different time points, and values indicate means ± SEM. The normalized dark preference (percent of time period) scatter plots of significance comparison were -72-hour to -24-hour and +24 hour to +72-hour time points (Fig. 4 g, values indicate means ± S.E.M.) which showed the distribution of the place-preference assay for WT (n=10), TREK1 KO (n=9), and TREK1 KO mice didn't show any significant different between the before period without heating and the after period with MNP injection with AMF heating, and WT significantly decreased the percent of time spent in the dark area between before without heating and after

MNP injection with AMF heating. Similar results were seen for the before-after effects of the average of each mouse's dark preference on the percentage in the dark for the WT and TREK1 KO mice with and without magnetothermal stimulation (Fig. 4 h). These results are consistent with the previous scatter spot plots and before-after plots. In addition, on the one hand, our data showed the dark preferences during the pre-field which are very similar for both WT and TREK1 KO mice (Supplementary information Fig.3 a and b), and the dark preference had a significant difference which is already shown in Fig. 4 e, f, g and h and also in Supplementary information Figure.3 a and b, but this kind of dark preference has some degree of memory effects during the post-field in Supplementary information Figure.3 a and b. On the other hand, our mice excursion number (going in and out frequency) in the dark also illustrated that WT mice were frequently trying to get out of the dark area during magnetothermal heating than the TREK1 KO mice after MNP injection (Supplementary information Fig.3 c and d), then these results are also consistent with the histogram results from WT (significant short time interval between mouse escaping the dark area after magnetothermal stimulation, Supplementary information Fig.4 c and d) and TREK1 KO mice (no significant change before and after magnetothermal stimulation) (Supplementary information Fig.4 a, b, c and d). Furthermore, both WT and TREK1 KO mice showed a very similar normalized excursion number from the left sided light area (1/3 of the whole area) or the right light side (1/3 of the whole area) of the entire light area which gradually dropped down from the pre-field duration to the during-field duration and post-field duration without MNP injection (Supplementary information Fig.3 e, f, g, and h). This result inferred that both WT and TREK1 mice have similar characteristics and fewer excursions for new environment exploration over time. After the behavior experiments, neural activity was inspected by C-Fos quantification of immunostaining of the VTA area for both WT and TREK1 KO mice, thus we didn't find any difference between WT and TREK1 KO mice, resulting in a significantly higher proportion of C-Fos–positive (C-Fos^{+}) cells when mice were in the dark rather than in the light area for WT mice (Fig.3 d and e), as revealed by a two-way analysis of variance (ANOVA) with a Bonferroni post-hoc test.

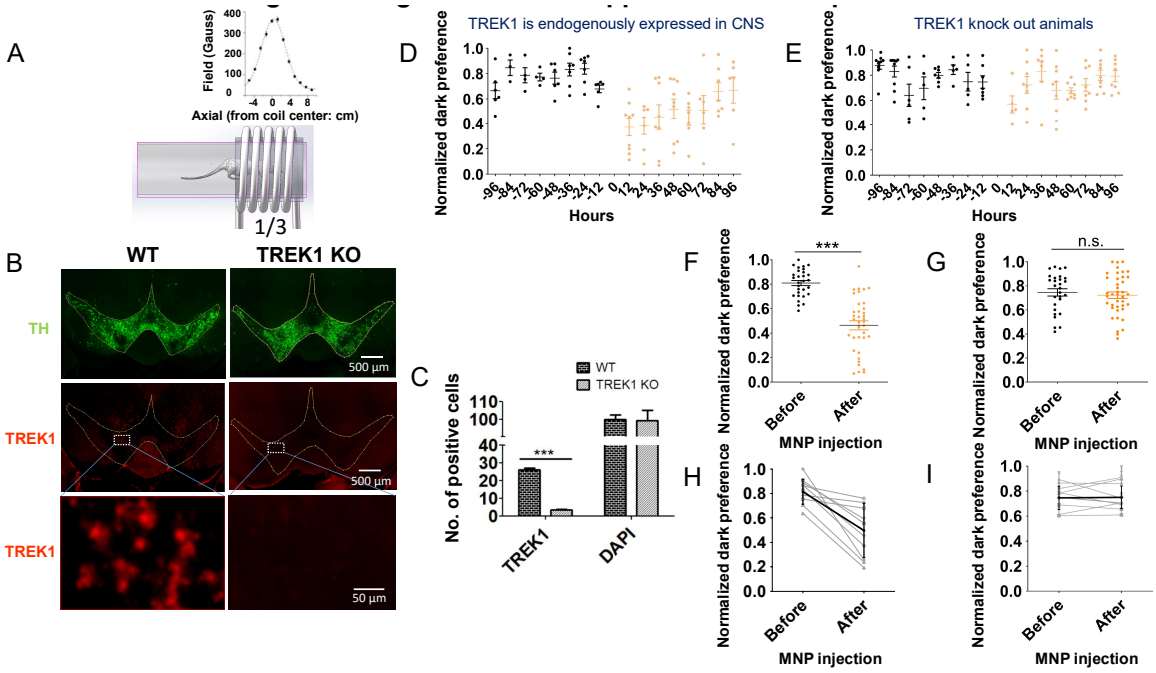

Figure 5: ***Magneto-thermal suppression of dark preference*** **(A)** Representative GCaMP6s fluorescence changes of neuronal activity of the basal, ethanol activation stimulation,

and acute magnetothermal silencing with fiber photometry recording in real-time (4 traces from 2 mice). Typical neuronal activity of VTA dopamine neurons recovery of post 15 minutes of silencing duration. **(B)** Quantification of scatters plot of different neuronal activity states: basal, ethanol activation stimulation, magnetothermal silencing, and recovery in the acute ethanol stimulation. **(C)** Left: schematic diagram of magnetothermal stimulation social interaction chamber with a satellite launch room, the recorded mouse located in the vertical chamber in magnetic coil, and another same-gender novel mouse release in the satellite chamber. Right: schematic diagram of video tracking the trajectory of the mouse. **(D)** The typical mouse appears in front of the mouse recorded by Fiber photometry and the real-time Neurons' activity signal without the mouse's social stimulation**. (E)** Multiple mice can repeat the signal activation of the neuronal population in the VTA brain region after typical social stimulation in mice. **(F)** Typical magnetothermal silencing the signals during the social stimulation in the gray shadow magnetic field on durations. **(G)** Quantification of scatter plot of different neuronal activity states: basal, social interaction stimulation, magnetothermal silencing in the acute ethanol stimulation.

359 **Discussion**

360 This study answered a recent call for solid and focused scientific research to guide neuronal activity research
361 after silencing a dynamic circuit or particular neuronal system with related initiatives[3]. Current global
362 research of silencing neuronal activity is limited in utilizing optogenetics and chemogenetics methods.
363 Obviously, these technologies have their advantages; for example, optogenetics allows much better spatial
364 resolution, typically provides information from more than one cell, thus significantly increasing the
365 throughput. Chemogenetics is less invasive and more flexible as it relies on designer ligands that can be
366 simply introduced by injection. However, the characteristics of these strategies severely limit their
367 application in biomedical research since these mainly showed that the optical fiber connection of
368 optogenetics makes complex behavioral research impossible. The low temporal resolution of
369 chemogenetics corresponds to the rapid response and to changes of the nervous system, which cannot meet
370 the needs of rapidly comparable dynamic circuits and freely moving behavioral research. Optogenetics
371 cannot be applied in other clinical applications since fiber implantations, and chemogenetics also have
372 limitations of a too low temporal resolution and the strong side effects of drugs. Here, we present a
373 magnetothermal strategy for silencing neuronal activity with a TREK1 ion channel, and this TREK1 unique
374 character for silencing the neuron is temperature rate-independent, and TREK1 is widely expressed in the
375 human body.

376 For cellular silencing of hippocampal culture neurons, although the channel is known to be not as
377 thermosensitive as TRPV1 and Anoctamin1, we found that TREK1 overexpression neurons respond
378 strongly to temperature ramps. Our research results showed the overlap of bath temperature ramp and
379 GCcaMP6f firing from a rat hippocampal neuron. When the temperature is ramped, the cell ceases to fire
380 as the temperature increases, when it would be otherwise firing. This silencing effect is dramatic, and it can
381 be repeated. Since hippocampal neurons are already known to express the TREK1 ion channel highly, when
382 we ramped the buffer temperature in a relatively low expressed TREK1 in WT neurons, the silencing effect
383 was observed as well; it was not as drastic as in the overexpression of cells. Therefore, we can infer that
384 this silencing involves TREK1. Our data also suggest that the TREK1 thermal sensitive ion channel can be
385 used to silence the neurons with a high temporal resolution and fast response with a delay since the heating
386 starts at 0.9 seconds for TREK1 overexpression and ~2.9 seconds in WT, which has a relatively lower
387 expression of TREK1 than TREK overexpression ones. Besides, the thermal sensitive TREK1 is temperate
388 rate dependent, meaning it does not need a high absolute temperate to activate the silencing.

389 In this study, we first realized measurable local heating *in vivo*. Previous studies have eluded local heating
390 using the magnetothermal method because of this challenge, and our membrane binding technology needs
391 professional biochemical synthetic optimization technology. This local heating needs professional and

392 precise injection in the location for the bulky volume injection of MNPs; notwithstanding this limitation,
393 this study suggests performing a precise injection. However, this problem could be solved if we consider
394 adopting a precise stereotaxic apparatus with an adjustable angle arm or image-guided MNP injection
395 technology by micro-CT.

396 We also found that heating injected with MNPs is volume-dependent, and repeated injections after the
397 effect subsided several weeks later are possible when heating is regained; these repeat injections on
398 consecutive days can deliver more MNPs achieve higher heat. Bulky injection allows the MNPs to reside
399 in the particular brain region for several weeks, even several months, making it possible for longitudinal
400 magnetothermal stimulation in the deep brain at any time with a single MNP injection. In addition, our
401 MNP injection concentration (<20mg/mL) and volume (<1.8uL) for the angle bulk injection and MNP
402 injection concentration (<4mg/mL) and volume (<1.2uL) were made for antibody binding and targeting a
403 particular neuronal population. The concentration and volume are decreased much lower than in the
404 previous study (100mg/ml, 2.5uL)[7], so these improvements have much less impact on brain damage.
405 Simultaneously, angle injection avoids the bulky volume black MNPs blocking GCamp7f signal between
406 the fiber tip and GCamp7f expression area. We did not examine the biocompatibility and toxicity test again
407 since our injection volume much less than previous research, and animal behavior also demonstrates regular
408 activity and behavior after MNP injection. We verified the MNPs' influence by checking the sham group
409 for saline (data not shown here).

410 Our dark/light conditioned place preference (CPP) behavior test implied that the dopamine (DA) neurons
411 have more activity in the dark than in the light area where the mouse is located in the dark, and C-Fos
412 histology revealed much more positive C-Fos cells (more activity in the VTA region, when the mouse is
413 located in the dark area than light area) in a long period timecale; our fiber photometry recording results
414 for calcium imaging further showed that DA-neurons have high activity when the mouse switches from the
415 light to the dark area (Fig. 3 a, b, and c), although this high activity doesn't last for the entire dark period.
416 We think it is a rapid response of transient changes from DA neurons' responses to dark and light states.

417 Out acute *in vivo* magnetothermal stimulation can clearly indicate that our manipulating the silencing of
418 DA neurons is possible in dynamic circuits and complex biological systems through the TREK1
419 temperature ion channel. This silencing method will provide a new and effective way to isolate neural
420 circuits in preclinical research in systemic neuroscience research of specific neuronal populations or circuits.

421 In future research, bi-direction silencing and activation for two different neuronal populations or different
422 brain regions and reversible silencing for the same neuronal population with conditional gene knockout
423 thermal sensitive ion channels should be done. For local heating research consideration, the local ultrasound

424 heating for thermal activation or silencing for neuronal activity research could be a new direction. Besides,
425 we will apply these techniques to different disease models. The ultimate goal is that these technologies can
426 achieve clinical transformation shortly with more than hundreds of kinds of nanoparticles which the FDA
427 approved in the past few years[24]

428

429

430 **Materials and Methods**

431 **Animals**

432 Male and female C57BL/6 mice wild-type (WT) (Jackson Laboratory, #000664), DAT: Cre mice (Jackson
433 Laboratory, #006660), and C57BL/6 background TREK-1$^{-/-}$ knockout (KO) mice were obtained from Dr.
434 Andreas Schwingshackl (Ronald Reagan UCLA medical center, UCLA Mattel Children's hospital), while
435 prague Dawley rats were used for cell culture. All of the animals aged 10-12 weeks were housed four per
436 cage and maintained under controlled temperature (23 ± 3 °C) with a reverse 12-hr light/dark cycle and
437 provided standard rodent chow and water available ad libitum during the duration of the experiments. The
438 animals were acclimatized for seven days before experiments and habituated to handling for at least three
439 days before behavioral testing; for other experiments, the animals would return to the animal room after the
440 experiments on the same day. All experimental procedures for animal care and use were approved by the
441 State University of New York at Buffalo Committee on Animal Care and followed the National Institutes
442 of Health Guide for the Care and Use of Laboratory Animals.

443 **Cell culture and cellular level thermal silencing**

444 *Preparation of neurons*

445 For dissociated hippocampal neuron culture preparation, hippocampal neurons were harvested from
446 embryonic day 17 (E17) Sprague Dawley fetuses. Briefly, dissected hippocampal tissue was digested with
447 50 units of papain (Worthington Biochem) for 6 min at 37 °C, and the digestion was stopped by incubation
448 with ovomucoid trypsin inhibitor (Worthington Biochem) for 4 min at 37 °C. Tissue was gently dissociated
449 with Pasteur pipettes, and dissociated neurons were plated at a density of 20–30K per glass coverslip coated
450 with Matrigel (BD Biosciences), and the neurons were placed in Tyrode's solution (Sigma Aldrich). After
451 cell adhesion, an additional plating medium was added. Neurons were grown at 37 °C and 5% CO_2 in a
452 humidified atmosphere. After transfection or nucleofection, the neuronal cultures were placed in the
453 incubator for the next 24-48 hours to express the proteins (GCaMP6f or TREK1). During this time, 1 μM
454 TTX (Tetrodotoxin) was added to the neuronal culture to minimize endogenous activity. The TTX was

455 washed out during imaging and then transfected *in vitro* on days 6-8 (DIV 6–8). The imaging buffer also
456 contained synaptic blockers DLAP-5 25 μM, NBQX 10 μM, Gabazine 20 μM, and the osmolality was
457 adjusted to 310-315 mosmole/L. All measurements on neurons were taken after DIV 16.

458 *Targeting nanoparticles for the neurons*

459 Nanoparticles were targeted to the neuronal cell membrane via biotinylated A_2B_5 antibody (433110,
460 Invitrogen). Neuronal cultures grown on a 12 mm diameter coverslip were loaded in the imaging chamber
461 (ALA scientific), holding 150 μl of the imaging buffer (PH 7.3). Biotinylated antibody (2 μg/ml) was added
462 and incubated for 10 minutes before being washed off by perfusion with HEPES buffer (PH 7.3).
463 Neutravidin conjugated nanoparticles were added at 10 μg/ml, and after 5 minutes, the unbound
464 nanoparticles were washed off. The local temperature rise near the nanoparticles was measured by
465 fluorescence intensity changes of a DyeLight 550 fluorophore integrated in the NeutrAvidin coating.

466 *Recording magnetothermal neuronal membrane heating*

467 Fluorescence microscopy of membrane decorated nanoparticle bound dye was done with an inverted
468 epifluorescence microscope (Zeiss Axio Observer A1M). The alternating magnetic fields (AMFs) induce
469 eddy currents in the metallic microscope objective and heat the nanoparticles. The fluorescence intensities
470 of molecular fluorophores are sufficiently temperature-dependent to provide a molecular scale thermometer.
471 The membrane-bound nanoparticles heated with an area density-scaling factor were calibrated (1.1×10^{-3} ±
472 6.7×10^{-5} °C.μm^2/s).

473 *Recording the cultured neuron silencing by bath/magnetothermal heating*

474 We collected the cultured neurons' spike in dissociated rat hippocampal cultures with significantly
475 decreased magnetothermal temperature ramps and absolute temperature increase. The activity data were
476 recorded on wild-type (WT) rat hippocampal neurons and TREK1 overexpressing rat neurons.

477 **Stereotaxic surgeries**

478 TREK1 knockout (KO) or wild type (WT) mice of 10-12 weeks of age were given isoflurane anesthesia
479 before being laterally injected with premixed 0.5 uL Gcamp6f (*AAV5.Syn.GCamp6f.WPRE.SV40*) and
480 TREK1 (*rAAV9/PAAV-hysn-TREK1*) in the VTA region (VTA, coordinates: -3.3 mm AP, ±0.4 mm ML, -
481 4.5 mm DV, AP -Anteroposterior. ML - Mediolateral. DV - Dorsoventral), as well as the DAT: Cre mice
482 were injected in the VTA with GCamp6f (*AAV5.syn.flex.GCamp6s.WPRE.SV40*). ML and AP coordinates
483 are relative to Bregma, and DV coordinates are relative to the dura mater. Hence injection was slowly
484 performed with a microinjection pump (UMP3, UMC4, World Precision Instruments, Inc., Sarasota, FL,

485 USA) at the speed of 60 nL/min with a 31-gauge needle; after virus injection, the needle was left in place
486 for 10 minutes before slowly retracting it.

487 **Stereotaxic cannula implantation**

488 The experimental mice were individually anesthetized with isoflurane and underwent surgery, were
489 mounted in a stereotaxic device, and their head was secured. Before surgery, Buprenorphine (0.1mg/Kg)
490 was administered routinely through an SC injection. Before drilling the hole at the VTA coordinates, ensure
491 that the skull is carefully leveled via DV coordinate measurements. The implanted fiber needs to be
492 connected to the scientific camera and check the increasing signal during the slow implantation of the fiber
493 down to the VTA area. The fiber can be fixed after finding the maximum signal increase above the top part
494 of the VTA (optical fiber implants were placed above the VTA; usual DV depth is between 4.0-4.3 mm)
495 and then glued with Vetbond adhesive around the surgical skin incision. After drying, apply C&B Metabond
496 where the dental cement will contact the skull, and finally, apply several layers of dental cement to affix
497 the fiber onto the skull. Ensure that the mouse is on a heating pad to maintain its body temperature during
498 surgery; after surgery, return the mouse to its home cage when the mouse is fully awake. Carprofen (5mg/kg)
499 was administered once daily subcutaneously for two days.

500 **Stereotaxic angle injection for magnetic nanoparticles (MNPs)**

501 The mice underwent stereotaxic bulky volume MNP injection (core-shell: $CoFe_2O_4$-$MnFe_2O_4$ ~14nm
502 diameter or Magnetite: spherical Fe_3O_4~22nm, 10mg/ml, 1.2uL) in the VTA with the coordinates of (-3.3
503 mm AP, 0.4 mm ML, 4.8 mm DV) with a 27-gauge needle. We adopted the membrane-binding injection
504 to locally heat the brain cell membrane in live mice, or we stereotaxically injected A_2B_5 antibody (1mg/ml,
505 0.6ul) into the region of interest. The injection was followed by MNP (2mg/ml, 0.6uL) injection into the
506 same spot. The injection speed was a constant 60 nL/min (UMP3, UMC4, World Precision Instruments,
507 Inc., Sarasota, FL, USA). Nanoparticles attached to neurons in the brain showed heating for at least 7 days
508 for the membrane binding method, and the volume injection lasted for 1-2 months. For both of these
509 injection methods, the needle was parallel to the sides of the ferrule of the fiber, and then the drill was
510 mounted into the stereotaxic device. Gently drill a hole through the dental cement with a 16-degree angle
511 with the fiber in the front-rear plane, vertical with the coronal plane (16-degrees from rear to front in the
512 vertical direction). Then, mount the needle drawn with 1.2uL MNPs, slowly go down the predetermined
513 coordinates of (-3.3 mm AP, 0.4 mm ML, 4.8 mm DV) and inject the MNPs slowly into the edge of the
514 VTA region or the Gcamp6 expression area (injection speed, 20nL/min for volume, and 60 nl/min for

515 membrane binding). The needle was retracted slowly and waited for a 10-minute interval after every
516 withdrawal of 0.5mm.

517 **Fiber Photometry setup**

518 The reconfigurable dichroic mirrors were mounted in removable dichroic filter cage cube holders (CM1-
519 DCH, THORLABS) that enabled two different light sources: one fluorescence excitation 470 nm LED light
520 source (M470F3, THORLABS) to be coupled with fiber optic SMA patch cables (M28L01, Ø400 µm, 0.39
521 NA, Low OH, THORLABS) and a corresponding collimator. In this configuration, a 470-nm LED filtered
522 with a 470-nm bandpass filter (Thorlabs, FB470-10) was fiber-coupled into the dichroic cube holder and
523 another LED light source 405nm beam (M405F1, THORLABS) with a 405-nm bandpass filter (Thorlabs,
524 FB405-10) was coupled in the same way with another collimator (Thorlabs, F671SMA-405 and AD11F)
525 and a 495nm long pass dichroic mirror (Semrock, FF495-Di02-25 ×36). The excitation LED light produced
526 an excitation spot with a ~2.5-mm diameter at a working distance of a 20×/0.40-NA objective (Olympus,
527 PLAN 20×), and the objective was fixed on a framed stage. A 400-µm-diameter 0.50-NA fiber
528 (THORLABS, FP400ERT) was used to transport fluorescence excitation. One end of the fiber terminated
529 in an FC/PC multimode connector with a ceramic ferrule (Thorlabs, 30440C1) was fixed on 3-axis
530 MicroBlock compact flexure stages (THORLABS, MBT616D) at the working distance of the objective,
531 and the other end terminated in 1.25-mm-diameter ceramic ferrules (CLFC 440). This ferrule was coupled
532 via a ceramic sleeve (Thorlabs, ADAL1) to a 1.25-mm-diameter ferrule implanted into a mouse head.
533 Fluorescence emission from the fibers was passed through a 520nm bandpass fluorescence emission filter
534 (selected for GCaMP6 recording; Semrock, FF01-520/35-25). The fluorescence image was focused onto
535 the sensor of an sCMOS camera (Andor, Zyla 4.2PLUS) through a tube lens (Thorlabs, AC254-040-A-
536 ML)[25].

537 The excitation GFP 470nm LED light and the correcting motion-related artifacts present in the 405-nm
538 isosbestic wavelength were applied as a 50ms/50ms switching mode, and switching LED lights were
539 controlled by LED drivers (LEDD1B, THORLABS) through Clampex software (V10.7.03, Molecular
540 Device, LLC) and AXON CNS Digidata 1440A hardware (Molecular Device, LLC). The camera sampling
541 frequency was set at 100 Hz and can evenly collect 5 data points during each switching period and utilize
542 the middle three points for the data processing. The 470 nm and 405 nm signals were separated with the
543 threshold, which was determined from the gap of the 470 nm and 405 nm values.

544

545 **Alternating magnetic fields (AMF) of the magnetothermal system setup**

546 Thermal sensitive ion channels respond to the alternating magnetic fields (AMFs) stimulus. A customized
547 magnetothermal system generates the AMFs (30 KA/m) in the low radio frequency regime (400KHz, 10
548 kHz-1 MHz adjustable), which can penetrate arbitrarily deep regions of the brain and interact minimally
549 with biological tissues. On the other hand, magnetic nanoparticles (MNPs) were injected into the particular
550 brain region in the mouse, where the MNPs were exposed to AMF dissipated heat and thus can trigger heat-
551 sensitive ion channels. We functionalized magnetic nanoparticles for bio-conjugation to the cellular
552 membrane or volume injection for suspension in brain tissue to utilize this. Therefore, the particular neuron
553 population or brain region will achieve the absolute temperature or temperature rate heating during the field.

554 ***In vivo* measurement of local heating via GCamp7f signal using fiber Photometry**

555 Measurement typically starts 24 hours after MNP injection. The experimental mouse was deeply
556 anesthetized with isoflurane for 40 minutes in the induction box with 2-2.5% isoflurane; the implanted
557 ferrule with a fiber glued in it was then placed the site of nanoparticle decoration. This serves as a port to
558 which the photometry fiber can be connected repeatedly during experiments. For all experiments, the mice
559 were anesthetized and placed within the hyperthermia coil, connected to the primary fiber, which is already
560 connected to the fiber photometry, and then put the mouse into the U shape magnetic coil and make sure
561 the mouse head is in the middle of the coil height. The data collecting period needs the room to be dark or
562 cover the fiber photometry and fiber connecter with a black cloth to avoid light from outside. During the
563 recording, the 470 and 405 nm LED lights to need to be turned on according to the Clampex software
564 protocol, and then start recording the data from the Andor Zyla camera for the required time. Finally,
565 analyze the data and convert it to the temperature increasing curve using the calibration data. A typical
566 measurement session lasted about half an hour, after which the animals quickly recovered and were returned
567 to their home cage.

568 **Calcium imaging recording of the neuron's activity through fiber Photometry**

569 Imaging typically started two weeks after fiber implantation surgery and 12-24 hours after MNP injection.
570 Mice were lightly anesthetized (0.7-1% isoflurane), then connect the fiber to the ferrule which was
571 implanted into the mouse brain, gently move the mouse into the U magnetic coil and wait for 40 minutes
572 until the mouse is completely awake (no isoflurane effects), and check the mouse's regular activity and
573 behavior. Similar to the operation of local heating, the recording of neural activity was performed with the

574 awake mouse, start recording the neural activity, click the Clampex recording button to start the LED light
575 as in the 50/50 ms switching protocol, and then start recording the data using the Andor Zyla camera for 5
576 minutes or other periods. A typical recording session lasted around half an hour, after which the animals
577 were returned to their home cage.

578 **Conditioned place preference (CPP) behavior**

579 The animals were acclimatized for 3 hours before the experiments and habituated to handling for at least
580 three days (pre-training, twice per day) before the behavioral test. The CPP behavior chamber was covered
581 in black for one-third of the total length, and the black covered part was set in the magnetic coil and exposed
582 to the AMFs during the field on, and then performed on the mice in the behavior chamber, where the
583 experimental mouse is freely moving in the chamber for 20 min, and applied AMFs during the middle 10
584 minutes, and the first 5 minutes and the last 5 minutes when the AMF was kept off state. The behavior test
585 was repeated from -96 hours to 0 hours with twelve-hour intervals, and then the mice were given a
586 stereotaxic nanoparticle injection (core-shell: CoFe2O4-MnFe2O4 ~14nm diameter or Magnetite: spherical
587 Fe3O4~22nm) in the VTA with the coordinates of (-3.3, 0.4, 4.8 mm) at a 16-degree angle with a 27-gauge
588 needle. Following the nanoparticle injection, mice underwent 0 to +96 hour CPP experiments with the same
589 twelve-hour intervals. These CPP behavior tests were designed for different groups of WT mice (n=10) and
590 the TREK1 KO mice (n=9) with different TREK1 expression levels in the VTA region. The light-dark
591 chamber only light area was illuminated by the flat LED light, and light area activity was adopted with the
592 entire light chamber, which was illuminated with the flat LED light. The mouse remained in space for 20
593 min/trial, and was trained three times with the trained interval of 12 hours to eliminate the spontaneous
594 exploratory behavior in a novel environment, the mouse mostly spent time in the dark area (sacrificed the
595 mouse to maintain the dark state in 60-90 minutes), and performed subsequent C-Fos staining for the dark
596 training and C-Fos assay. In addition, another entire bright chamber was used for both WT and TREK1 KO
597 mice to test the brightness preference (number of excursions from 1/3 of the bright area of the entire bright
598 area normalized in 5 minutes) compared with the dark preference (number of excursions from 1/3 of the
599 dark covered chamber), and number of excursions from the bright/dark area during the previous field,
600 during field heating, and after the field was normalized per 5 minutes.

601 **Acute *in vivo* magnetothermal silencing during ethanol activation and social interaction**

602 To achieve dramatic silencing effects from hyperactive neurons after applying magnetothermal silencing
603 for in vivo mouse we activated neuronal activity through ethanol administration or social interactions, and
604 we verified the acute magnetothermal silencing effects after ethanol activation or during social interactions.

605 All of these mice were used the TREK1 OE in VTA (premixed AAV5.Syn.GCamp6f.WPRE.SV40 and
606 rAAV9/PAAV-hsyn-TREK-1) for both of these acute in vivo magnetothermal silencing experiments.

607 *Ethanol activation and magnetothermal silencing*

608 Ethanol stimulates the firing activity of midbrain dopamine (DA) neurons, leading to enhanced
609 dopaminergic transmission in the mesolimbic system through intake from the mouse's mouth. Ethanol has
610 been shown to enhance the intrinsic pacemaker activity of DA neurons directly; this activation provides us
611 with further magnetothermal silencing, and this silencing can be easily observed through the in vivo fiber
612 photometry recording. TRE1 OE mice were used in these magnetothermal experiments (mixed the TREK1
613 virus and GCamp6f virus, which were injected into the VTA). For ethanol activation and silencing, the
614 subject mouse was located in the vertical coil, and we started to record the neuronal activity in the VTA
615 through fiber photometry. Secondly, apply ethanol, so it is absorbed into the mouse's mouth. About 5
616 minutes later, apply AMF to perform the magnetothermal silencing for this ethanol activation and record
617 all the processes.

618 *Social interaction activation and magnetothermal silencing*

619 Similarly, we also activated the neuronal activity by social interactions, and this can realize the social
620 interactions in the chamber around the subject mouse (mixed TREK1 virus and GCamp6f virus were
621 injected into the VTA) with fiber photometry real-time recording and allow the same gender mouse to be
622 released from the satellite chamber. Correspondingly, we recorded magnetothermal silencing during the
623 activated duration of social interactions. Therefore, we can observe dopamine neuron activity changes
624 between the social interactions without magnetothermal stimulation and the magnetothermal silencing with
625 AMF was executed during these social interactions.

626 **Immunohistochemistry**

627 Mice were overdosed with Ketamine/Xylazine and perfused transcardially with cold PBS, followed by 4%
628 paraformaldehyde (PFA) in PBS. Brains were extracted from the skulls and kept in 4% PFA at 4 °C
629 overnight and then 30% sucrose for 48 hours. Sixty-micrometer coronal slices were taken using a vibrating
630 slicer (Compresstome VF-200, Precisionary Instruments, Natick, MA, USA) and collected in cold PBS.
631 For immunostaining, each slice was placed in PBST (PBS + 1% Triton X-100) with 5% normal horse serum
632 for 3 h and then incubated with primary antibody at 4 °C for 72 h (rabbit anti-C-Fos 1: 2,000, cell signaling;
633 rabbit anti-Tyrosine Hydroxylase (anti-TH) 1: 2,000, Novus; Guinea pig Anti-KCNK2 (TREK-1) 1:200,
634 Alomone Labs, Rabbit anti-GABA (A) α Receptor 1:400, Alomone. Slices then underwent three washes
635 for 20 min each in PBS, followed by 3 h incubation with secondary antibodies (1:500 AlexaFlour488

636 donkey anti-sheep, (lot#139298) Jackson ImmunoResearch; 1:200 CY5 (for GABA) donkey anti-rabbit,
637 (lot#138569) Jackson ImmunoResearch) and 1:500 CY3 donkey anti-Guinea pig, (lot#134844) Jackson
638 ImmunoResearch). Following another 3 washes with PBS, the brain slices were transferred onto glass slides
639 and mounted with a mounting medium (VECTASHIELD containing DAPI nuclear stain) followed by
640 mounting and coverslipping onto microscope slides. Some clear, colorless nail polish was used to seal the
641 edges of the coverslips.

642 **Confocal imaging**

643 Fixed slice confocal imaging was performed on a Leica TCS SP8 confocal microscope and Leica DMi 8 at
644 Jacobs School of Medicine and Biomedical Sciences of the University at Buffalo microscopy facility.

645 **Statistics**

646 To evaluate statistical significance, data were subjected to a Student's *t*-test or ANOVA, and in the CPP
647 behavior experiments, the investigators were blinded to the different mouse genotypes. Statistical
648 significance was set at $P \leq 0.05$. All data are presented as means ± S.E.M. unless noted otherwise.

649 **AUTHOR CONTRIBUTION**

650 J.L. performed behavioral, biochemical, and imaging experiments, analyzed the data and wrote the paper;
651 R.M. performed cell culture imaging and partial behavior experiments and analyzed the data. M.H.
652 participated in some behavioral experiments and analyzed the data. S.P performed genotyping
653 experiments and partial imaging experiments. A.P. designed the experiments, supervised the project, and
654 wrote the paper.

655 **ACKNOWLEDGEMENTS**

656 We thank Dr. Andreas Schwingshackl for sharing the TREK1 KO mice with us. We thank Wade J.
657 Sigurdson for the excellent technical support of confocal imaging from the Jacobs School of Medicine
658 and Biomedical Sciences of the State University of New York at Buffalo. We also thank Denise Ferkey
659 for the support of the Wide-field fluorescence microscope from the Department of Biological Sciences of
660 the State University of New York at Buffalo. This work was supported by the grant from the National
661 Institutes of Health (MH094730) to A.P.

662 **Conflict of Interest**

663 None declared.

664 **References**

665 1. Zhang, F. *et al.* Multimodal fast optical interrogation of neural circuitry. *Nature* **446**, 633–639
666 (2007).

667 2. Du, Y., Lu, Q. & Wang, R. Using interspike intervals to quantify noise effects on spike trains in
668 temperature encoding neurons. *Cogn. Neurodyn.* **4**, 199–206 (2010).

669 3. Wiegert, J. S., Mahn, M., Prigge, M., Printz, Y. & Yizhar, O. Silencing Neurons: Tools,
670 Applications, and Experimental Constraints. *Neuron* **95**, 504–529 (2017).

671 4. Zhang, F. *et al.* The Microbial Opsin Family of Optogenetic Tools. *Cell* **147**, 1446–1457 (2011).

672 5. Zhu, H. & Roth, B. L. Silencing Synapses with DREADDs. *Neuron* **82**, 723–725 (2014).

673 6. Munshi, R. *et al.* Magneto-thermal genetic deep brain stimulation of motor behaviors in awake,
674 freely moving mice. *Elife* **6**, (2017).

675 7. Chen, R., Romero, G., Christiansen, M. G., Mohr, A. & Anikeeva, P. Wireless magnetothermal
676 deep brain stimulation. *Science (80-.).* **347**, 1477–1480 (2015).

677 8. Munshi, R., Qadri, S. M. & Pralle, A. Transient magnetothermal neuronal silencing using the
678 chloride channel anoctamin 1 (TMEM16A). *Front. Neurosci.* (2018).
679 doi:10.3389/fnins.2018.00560

680 9. Schneider, E. R., Anderson, E. O., Gracheva, E. O. & Bagriantsev, S. N. Temperature Sensitivity
681 of Two-Pore (K2P) Potassium Channels. *Curr. Top. Membr.* **74**, 113–133 (2014).

682 10. Wiedmann, F. *et al.* Mechanosensitive TREK-1 two-pore-domain potassium (K2P) channels in the
683 cardiovascular system. *Prog. Biophys. Mol. Biol.* **159**, 126–135 (2021).

684 11. Ranade, S. S., Syeda, R. & Patapoutian, A. Mechanically activated ion channels. *Neuron* **87**,
685 1162–1179 (2015).

686 12. Maingret, F. *et al.* TREK-1 is a heat-activated background K+ channel. *EMBO J.* (2000).
687 doi:10.1093/emboj/19.11.2483

688 13. Dey, D. *et al.* A potassium leak channel silences hyperactive neurons and ameliorates status
689 epilepticus. *Epilepsia* **55**, 203–213 (2014).

690 14. Patel, A. J. *et al.* Inhalational anesthetics activate two-pore-domain background K+ channels. *Nat.*
691 *Neurosci.* (1999). doi:10.1038/8084

692 15. Heurteaux, C. *et al.* Deletion of the background potassium channel TREK-1 results in a
693 depression-resistant phenotype. *Nat. Neurosci.* **9**, 1134–1141 (2006).

694 16. Woo, D. H. *et al.* TREK-1 and Best1 channels mediate fast and slow glutamate release in
695 astrocytes upon GPCR activation. *Cell* **151**, 25–40 (2012).

696 17. Bourin, M. & Hascoët, M. The mouse light/dark box test. *Eur. J. Pharmacol.* **463**, 55–65 (2003).

697 18. Yu, Y., Hill, A. P. & McCormick, D. A. Warm body temperature facilitates energy efficient
698 cortical action potentials. *PLoS Comput. Biol.* **8**, (2012).

699 19. Huang, H., Delikanli, S., Zeng, H., Ferkey, D. M. M. D. M. & Pralle, A. Remote control of ion
700 channels and neurons through magnetic-field heating of nanoparticles. *Nat. Nanotechnol.* **5**, 602–
701 606 (2010).

702 20. Young, J. H., Wang, M.-T. & Brezovich, I. A. Frequency/depth-penetration considerations in
703 hyperthermia by magnetically induced currents. *Electron. Lett.* **16**, 358–359 (1980).

704 21. Carrey, J., Mehdaoui, B. & Respaud, M. Simple models for dynamic hysteresis loop calculations
705 of magnetic single-domain nanoparticles: Application to magnetic hyperthermia optimization. *J.*
706 *Appl. Phys.* **109**, 83921 (2011).

707 22. Danjo, T., Yoshimi, K., Funabiki, K., Yawata, S. & Nakanishi, S. Aversive behavior induced by
708 optogenetic inactivation of ventral tegmental area dopamine neurons is mediated by dopamine D2
709 receptors in the nucleus accumbens. *Proc. Natl. Acad. Sci.* **111**, 6455–6460 (2014).

710 23. Sun, F. *et al.* Adiponectin modulates ventral tegmental area dopamine neuron activity and anxiety-
711 related behavior through AdipoR1. *Mol. Psychiatry* **24**, 126–144 (2019).

712 24. Jones, A. A. D., Mi, G. & Webster, T. J. A Status Report on FDA Approval of Medical Devices
713 Containing Nanostructured Materials. *Trends Biotechnol.* **37**, 117–120 (2019).

714 25. Kim, C. K. *et al.* Simultaneous fast measurement of circuit dynamics at multiple sites across the
715 mammalian brain. *Nat. Methods* **13**, 325–328 (2016).

716